

# Edge-to-Edge Matching of Lattice Planes and Coupling of Crystallography and Migration Mechanisms of Planar Interfaces

J.F. NIE

The structure and migration mechanisms of planar interfaces are examined geometrically using the concept of edge-to-edge matching of lattice planes and the Moiré plane approach derived from this concept. The selected examples of planar interfaces include those associated with rational, near-rational, or irrational orientation relationships. It is demonstrated that the orientation and structure of planar interfaces associated with these orientation relationships can be rationalized by the Moiré plane approach, and that the migration of these interfaces in their normal directions can occur *via* successive nucleation and lateral gliding of growth ledges that are in the form of transformation disconnections, for low-index interfaces, and of Moiré ledges, for high-index interfaces. It is further demonstrated that a shear, and thus a shape change, is associated with the motion of all planar interfaces defined by the edge-to-edge matching of lattice planes.

## I. INTRODUCTION

THE structure and migration mechanisms of planar interfaces have received considerable attention and research in the last 50 years. While significant progress has been made so far on this topic, there are still some unsolved or controversial issues, particularly on the coupling of crystallographic features and the migration mechanisms of planar interfaces. It is the purpose of the present article to use the concept of edge-to-edge matching of lattice planes, and the Moiré plane approach<sup>[1,2,3]</sup> that is derived from this concept, to rationalize the orientation, structure, and migration mechanisms of planar interfaces that are either rationally or irrationally oriented with respect to the two lattices involved. For the purpose of comparison and straightforward discussion, and following the approach of Howe *et al.*,<sup>[4]</sup> the planar interfaces examined in this article include those that are associated with (1) rational orientation relationships, (2) near-rational orientation relationships, and (3) irrational orientation relationships. To avoid any confusion arising from terminologies, the term “irrational” refers to relationships that cannot be defined as rational or close to rational, *i.e.*, random. For simplicity, two-dimensional (2-D) lattices are used in the present analysis.

## II. ORIENTATION RELATIONSHIPS AND PLANAR INTERFACES

Suppose we have a 2-D matrix lattice that is defined by two sets of planes,  $m_x$  and  $m_y$ , that intersect with an angle  $\theta_m$ . For the coordinate system depicted in Figure 1, the normal of the  $m_y$  plane is parallel to the  $y$ -axis. If this lattice

is deformed by a simple shear, depicted by an angle of  $\theta$ , along the  $x$ -axis on the  $y$  plane and a uniaxial expansion of  $\eta_x$  in the  $x$  direction, then the plane  $m_x$  is transformed into plane  $p_x$ . If this lattice is further deformed by a uniaxial expansion of  $\eta_y$  in the  $y$  direction, then the plane  $m_y$  transforms into plane  $p_y$ , and a new lattice (named “product lattice”) is generated. If we define the angle between the  $p_x$  and  $p_y$  planes as  $\theta_p$ , then the shear angle is given by  $\theta = \theta_m - \theta_p$ . For the structural transformation described,

$$s = \tan(90 \text{ deg} - \theta_p) - \tan(90 \text{ deg} - \theta_m),$$

$$\eta_x = (d_{p_x} \sin \theta_m) / (d_{m_x} \sin \theta_p),$$

and

$$\eta_y = d_{p_y} / d_{m_y},$$

where  $d_{m_x}$ ,  $d_{m_y}$ ,  $d_{p_x}$ , and  $d_{p_y}$  are the interplanar spacings of the  $m_x$ ,  $m_y$ ,  $p_x$  and  $p_y$  planes, respectively. To achieve commensurate (coherent) matching of  $m_x$  and  $p_x$  planes and of  $m_y$  and  $p_y$  planes in an edge-on manner in a planar, if any, interface that separates the two lattices (Figure 1), the product lattice needs to rotate through an angle  $\varphi$ , with respect to the matrix lattice and about the  $z$ -axis; this angle is given by<sup>[3]</sup>

$\cos \varphi =$

$$\frac{(1 + \eta_x \eta_y)(\eta_x + \eta_y) + \sqrt{s^2 \eta_y^2 [s^2 \eta_y^2 - (\eta_x^2 - 1)(\eta_y^2 - 1)] + D [2s^2 \eta_y^2 - (\eta_x^2 - 1)(\eta_y^2 - 1)]}}{(\eta_x + \eta_y)^2 + s^2 \eta_y^2 + D}$$

[1]

where  $D = (\eta_x - \eta_y)^2 \tan^2 \gamma - 2s\eta_y (\eta_x - \eta_y) \tan \gamma$ , and  $\gamma = 90 \text{ deg} - \theta_m$ . The orientation of the coherent planar interface associated with this orientation relationship is defined by

J.F. NIE, Reader, is with the Department of Materials Engineering, Monash University, Victoria 3800, Australia. Contact e-mail: nie@eng.monash.edu.au

This article is based on a presentation made in the “Hume-Rothery Symposium on Structure and Diffusional Growth Mechanisms of Irrational Interphase Boundaries,” which occurred during the TMS Winter meeting, March 15–17, 2004, in Charlotte, NC, under the auspices of the TMS Alloy Phases Committee and the co-sponsorship of the TMS-ASM Phase Transformation Committee.

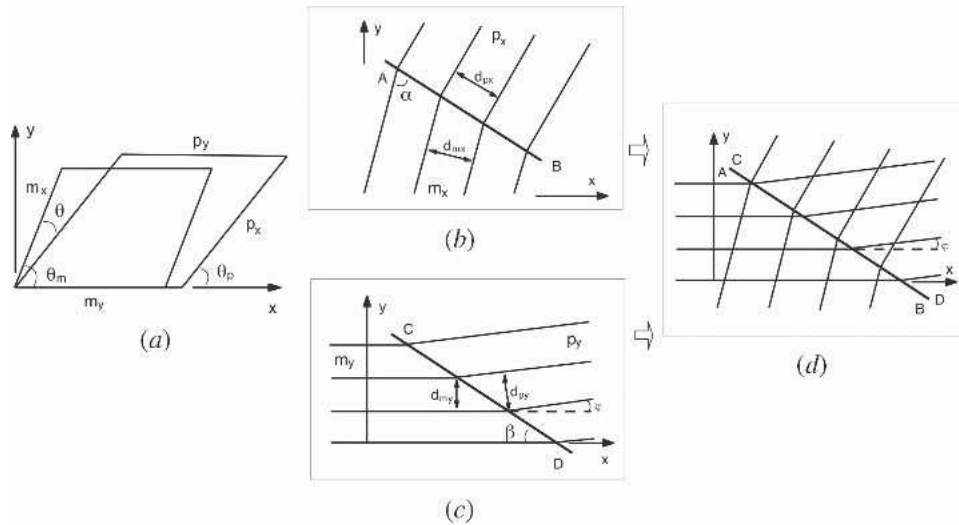


Fig. 1—(a) Schematic diagram showing two lattices that are related by a simple shear and a uniaxial expansion along the  $x$  direction in the  $y$  plane and a uniaxial dilatation in the direction normal to the  $y$  plane. (b) through (d) Geometric condition for achieving edge-to-edge matching of the  $m_x$  and  $p_x$  planes and of the  $m_y$  and  $p_y$  planes, in a single planar interface ( $AB//CD$ ) separating the two lattices.

$$\sin \alpha = \frac{s \cos \varphi + \sin \varphi (1 + \tan^2 \gamma + s \tan \gamma)}{\sqrt{s^2 + [(\eta_x - 1)(1 + \tan^2 \gamma) - s \tan \gamma]^2 + 2\eta_x(1 + \tan^2 \gamma)[(1 + \tan^2 \gamma + s \tan \gamma)(1 - \cos \varphi) + s \sin \varphi]}} \quad [2]$$

where  $\alpha$  is the angle between the interface plane  $AB//CD$  and the  $m_x$  plane. For structural transformations in which  $\theta_m > \theta_p$  ( $s > 0$ ), the rotation of the product lattice is clockwise (positive  $\varphi$ ), if  $\eta_x > 1$  and  $\eta_y < 1$  (or  $\eta_x < 1$  and  $\eta_y > 1$ ), or counterclockwise (negative  $\varphi$ ), if  $\eta_x > 1$  and  $\eta_y > 1$  (or  $\eta_x < 1$  and  $\eta_y < 1$ ). Note that, if the  $m_x/p_x$  pair and the  $m_y/p_y$  pair are defined as the two principal pairs, then the geometric condition specified by Eqs. [1] and [2] guarantees the matching of a group of lattice plane pairs that are derived from these two principal pairs. While  $m_x$  and  $m_y$ , or  $p_x$  and  $p_y$ , may represent any two planes of a lattice, they are often the closest-packed or near-closest-packed planes in the lattices involved in structural transformations.

For any structural transformations in which  $s \neq 0$ , the motion of the  $AB//CD$  planar interface in its normal direction will result in a shear displacement (shape change) of one lattice with respect to the other, if the commensurate edge-to-edge matching of lattice planes within this interface is to be preserved.<sup>[1,5]</sup> To preserve the continuity of the  $m_x$  and  $p_x$  planes across two adjacent planar interfaces, and any two opposing planar interfaces, the motion of the  $AB//CD$  planar interface requires the successive nucleation and lateral gliding of the Moiré ledges, within the interface, the unit height of which is defined by the interplanar spacing of the Moiré planes resulting from the intersection of the  $m_x$  and  $p_x$  planes, and is given by

$$h = \frac{d_{p_x} \sin \alpha}{\sin(\theta + \varphi)} \quad [3]$$

An inspection of Eqs. [1] and [2] and the schematic diagrams in Figure 1 reveal immediately the existence of planar interfaces that are associated with special ( $\eta_x = 1$ ,  $\eta_y = 1$ ,

or  $s = 0$ ) and general ( $\eta_x \neq 1$ ,  $\eta_y \neq 1$ , and  $s \neq 0$ ) cases of structural transformations. For the purpose of convenience and in the context of the edge-to-edge matching of lattice planes ( $s \neq 0$ ), the planar interfaces are classified into three major groups, as follows:

- (1) low-index interfaces associated with rational orientation relationships ( $\eta_x = 1$ ),
- (2) high-index interfaces associated with rational ( $\eta_x \neq 1$  and  $\eta_y = 1$ ) or near-rational ( $\eta_x \neq 1$  and  $\eta_y \neq 1$ ) orientation relationships, and
- (3) high-index interfaces associated with irrational orientation relationships.

### III. LOW-INDEX INTERFACES ASSOCIATED WITH RATIONAL ORIENTATION RELATIONSHIPS

If a structural change is such that  $\eta_x = 1$ , then  $\varphi = 0$  (Figure 2(a)). The orientation relationship between the two lattices is thus rational, with  $p_y // m_y$  and  $(p_x \wedge p_y) // (m_x \wedge m_y)$ . The planar product/matrix interface associated with this rational orientation relationship is invariably parallel to the  $m_y$  plane, irrespective of the value of  $\eta_y$  and  $s$ . Given that  $m_y$  and  $p_y$  are the closest-packed or near-closest-packed planes in each lattice and thus have low indices, the planar interface is, therefore, classified as a low-index planar interface, and it is fully coherent.

If there is no volume change in a structural transformation ( $\eta_x = 1$ ,  $\eta_y = 1$  and  $s \neq 0$ ), then the transformation strain itself (Figure 2(b)), and the corresponding shape change (Figure 3(a)), is a simple shear. The interfaces associated with the simple shear transformations include twin boundaries and symmetrical-tilt boundaries in homophase materials.<sup>[6-10]</sup> A unique feature of such planar interfaces is that they exist periodically in their normal directions, *i.e.*, there exists a set of such planes in their normal directions. In the case of  $\{111\}_f$  twin boundaries in face-centered cubic lattices, the spacing of the Moiré planes, defined by Eq. [3], is  $3d_{\{111\}_f}$ . It is now well understood that the continuous migration of a

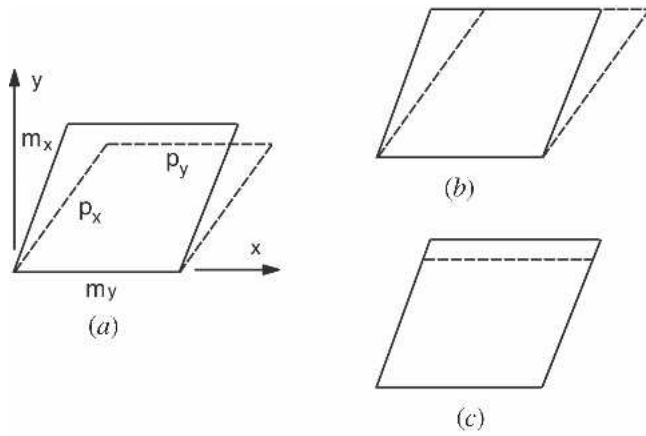


Fig. 2—Schematic diagrams showing structural transformations defined by  $\eta_x = 1$ : (a)  $\eta_x = 1$ ,  $\eta_y \neq 1$ , and  $s \neq 0$ ; (b)  $\eta_x = 1$ ,  $\eta_y = 1$ , and  $s \neq 0$ ; and (c)  $\eta_x = 1$ ,  $\eta_y \neq 1$ , and  $s = 0$ . The planar interface is parallel to the  $m_x$  plane in all three cases. Note that the case in (a) can be regarded as a combination of those illustrated in (b) and (c).

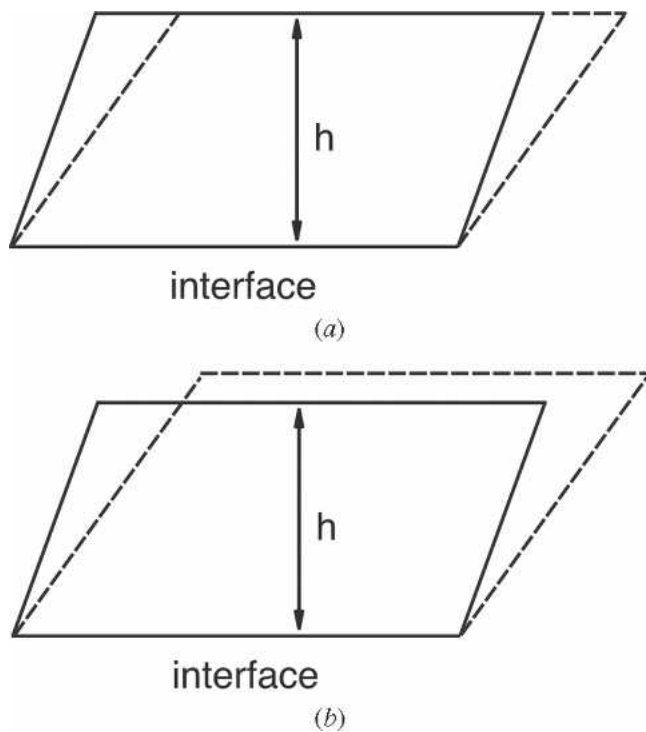


Fig. 3—Schematic diagrams showing the shape change representative of structural transformations defined by (a) a simple shear ( $\eta_x = 1$ ,  $\eta_y = 1$ , and  $s \neq 0$ ), depicted in Figure 2(b), and (b) a simple shear and a uniaxial dilatation ( $\eta_x = 1$ ,  $\eta_y \neq 1$ , and  $s \neq 0$ ), depicted in Figure 2(a). Height  $h$  is the interplanar spacing of Moiré planes defined by the intersection of the  $m_x$  and  $p_x$  planes. The dilatation strain normal to the interface is zero in (a) and is  $(\eta_y - 1)$  in (b).

twin boundary, as an entity, in its normal direction is energetically unfavorable, and that this normal migration of the twin boundary occurs *via* the successive nucleation and lateral gliding of ledges in the twin plane. Such ledges have been termed “transformation dislocations,”<sup>[11–14]</sup> “growth ledges,”<sup>[15,16]</sup> “disconnections,”<sup>[17,18]</sup> and “Moiré ledges.”<sup>[1]</sup> Existing experimental observations using high-resolution transmission electron microscopy indicate that the height of the ledges formed on twin boundaries is consistent with that

of Moiré ledges, *i.e.*,  $3d_{\{111\}_f}$ .<sup>[6,7]</sup> Note that ledges may also take the form of transformation disconnections with a smaller unit height, in order to minimize the shear displacement. The shear strain associated with a unit transformation disconnection is, however, identical to that of a Moiré ledge.

Most low-index planar interfaces are associated with transformations that have a combination of a simple shear and a uniaxial dilatation ( $\eta_x = 1$ ,  $\eta_y \neq 1$  and  $s \neq 0$ ) (Figure 2(a)). Such examples include  $\{111\}_\alpha$  habit planes of  $\gamma'$ ,  $\Omega$ , and  $T_1$  plates in Al-Ag,<sup>[19]</sup> Al-Cu-Mg-Ag,<sup>[20,21,22]</sup> and Al-Cu-Li<sup>[23]</sup> alloys, respectively;  $\{100\}_\alpha$  habit planes of  $\theta'$  plates in Al-Cu alloys;<sup>[24]</sup>  $\{1\bar{1}00\}_\alpha$  habit planes of  $\beta_1$  plates in Mg-Y-Nd alloys;<sup>[25]</sup>  $\{111\}_f$  habit planes of  $\varepsilon$  martensite plates in Fe-Mn-Si and Fe-Mn-Si-Cr-Ni alloys;<sup>[26,27]</sup>  $\{111\}_\gamma$  habit planes of  $\alpha_2$  plates in Ti-Al and Ti-Al-Ta alloys;<sup>[28]</sup> and planar interfaces separating  $\text{Ni}_3\text{Al}$  and  $\text{Ni}_3\text{Nb}$  lamellae in a Ni-Al-Nb alloy.<sup>[29]</sup> The planar interfaces associated with the exact Kurdjumow – Sachs, Nishiyama – Wassermann, Potter, and Pitsch – Schrader relationships, in which  $\eta_x = 1$ , can also be classified into this group.<sup>[2,3]</sup> Due to the volume change (caused by the simple dilatation) in the structural transformations, now there exists only a single planar interface, instead of a set of them, in which commensurate edge-to-edge matching of many pairs of lattice planes can be established, (Figure 3(b)). The formation of either a unit-height Moiré ledge or a unit-height transformation disconnection on this planar interface will cause an elastic distortion in the matrix or product lattice adjacent to the newly-formed planar interface, or both, as depicted in Figure 2 in Reference 30 and Figures 6 and 9 in Reference 17, if the coherent matching of lattice planes is to be preserved. In such cases, the interfacial defects may favor unit transformation disconnections to minimize the shear displacement. Given that any ledges formed on a fully coherent planar interface are not an intrinsic part of the interface structure, the lateral gliding of these ledges will not destroy the coherent matching of the two lattices.

Note that low-index planar interfaces can also be associated with structural transformations that can be defined by a uniaxial dilatation ( $\eta_x = 1$ ,  $\eta_y \neq 1$ , and  $s = 0$ ), as shown schematically in Figure 2(c). This uniaxial dilatation is equivalent to a uniform dilatation and a pure shear (simple shear plus rotation).<sup>[31]</sup> Examples of a uniaxial dilatation include  $\{001\}_b$  habit planes of HfN precipitates in nitrated Mo-Hf alloys,<sup>[32,33]</sup> planar interfaces in the exact Bain – Baker – Nutting, Pitsch, and Burgers orientation relationships.<sup>[2,3,34,35]</sup> A detailed description of such interfaces is beyond the scope of the present article.

#### IV. HIGH-INDEX PLANAR INTERFACES ASSOCIATED WITH RATIONAL OR NEAR-RATIONAL ORIENTATION RELATIONSHIPS

##### A. Interfaces Associated with Rational Orientation Relationships

For structural transformations in which  $\eta_y = 1$  (and  $\eta_x \neq 1$ ) (Figure 4(a)), the orientation relationship between the two lattices is again rational, with  $p_y/m_y$  and the matrix direction containing the  $m_x$  and  $m_y$  planes parallel to the product direction containing the  $p_x$  and  $p_y$  planes. Note that this orientation relationship is identical to that associated with  $\eta_x = 1$ . Similar to the case depicted in Section III, a set of parallel planar interfaces can exist between the two lattices, and commensurate edge-to-edge

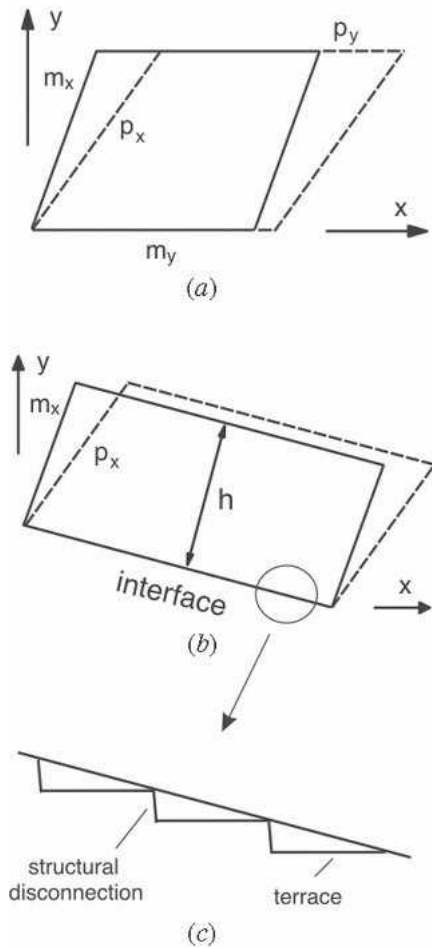


Fig. 4—(a) Schematic diagram showing the structural change defined by  $\eta_y = 1$ ,  $\eta_x \neq 1$ , and  $s \neq 0$ . (b) The high-index planar interface and the shape change associated with the structural transformation. Height  $h$  is the interplanar spacing of Moiré planes defined by the intersection of the  $m_x$  and  $p_x$  planes. (c) A section of the planar interface in (b), showing structural disconnections and terraces.

matching of many pairs of lattice planes can be established in each single planar interface of this set. The orientation of this set of fully coherent, planar interfaces is given by

$$\sin \alpha = \frac{s}{\sqrt{s^2 + [(\eta_x - 1)(1 + \tan^2 \gamma) - s \tan \gamma]^2}} \quad [4]$$

Note that each planar interface in this set is now not parallel to the  $m_y$  plane (Figure 4(b)), and thus has a high index, in general. Given that the  $p_y$  and  $m_y$  planes are parallel to each other and the planar interface is inclined to them, the macroscopic interface may also adopt a form that has a regular array of disconnections (or structural ledges) and terraces (Figure 4(c)). Note that these disconnections are different from those (transformation) disconnections formed on low-index interfaces, as they are now an intrinsic part of the interface structure, and only the synchronous motion of these disconnections can maintain the orientation and the structure of the interface. These disconnections are thus structural disconnections (or structural ledges),<sup>[16]</sup> rather than transformation disconnections, growth ledges, or transformation dislocations. (Ledges that are not an intrinsic part of the interface structure are defined as transformation dislocations, per References 11

through 14). In terms of the Moiré plane approach,<sup>[1]</sup> the migration of this type of planar interface involves the successive nucleation and lateral sliding of the Moiré ledges (or growth ledges) within the Moiré plane interface. The unit height of the Moiré ledges is defined by Eq. [3]. The structural transformations and the resultant shape changes in this group are equivalent to a simple shear (Figure 2(b)), with the shear direction parallel to the trace of the macroscopic planar interface (Figure 4(b)).

One example in this group is the structural transformation from orthorhombic or tetragonal to monoclinic in zirconia.<sup>[36–40]</sup> Characterization using *in-situ* transmission electron microscopy of the orthorhombic  $\Rightarrow$  monoclinic transformation in  $\text{ZrO}_2$  particles dispersed in  $\text{Nb}^{36}$  reveals a rational orientation relationship that is in the form  $(200)_m // (400)_o$ ,  $[0\bar{1}0]_m // [010]_o$ , and  $[00\bar{1}]_m // [001]_o$ . The planar interface associated with this orientation relationship is inclined at  $\sim 13.5$  deg with the  $(400)_o$  plane.<sup>[36]</sup> The crystallographic features, migration mechanisms of interfaces, and shape change associated with the orthorhombic  $\Rightarrow$  monoclinic transformation can be well accounted for by the Moiré plane approach. If we assume that the monoclinic lattice is generated from the orthorhombic lattice by shearing the orthorhombic lattice along the  $[001]_o$  direction in the  $(400)_o$  plane and expanding it in the  $[001]_o$  direction, together with an expansion in the  $[100]_o$  direction (Figure 5(a)), then

$$s = \tan(90 \text{ deg} - \theta_p) = \tan(\beta_m - 90 \text{ deg}),$$

$$\eta_x = d_{(002)_m} / (d_{(002)_o} \sin \theta_p) = c_m / c_o,$$

and

$$\eta_y = d_{(200)_m} / d_{(400)_o} = (2a_m / a_o) \sin \beta_m,$$

where  $a_o$ ,  $c_o$ ,  $a_m$ ,  $c_m$ ,  $\beta_m$  are lattice parameters of the orthorhombic and monoclinic lattices, respectively. If we further assume that  $a_o = 1.0166$  nm,  $b_o = 0.521$  nm,  $c_o = 0.511$  nm,  $a_m = 0.515$  nm,  $b_m = 0.521$  nm,  $c_m = 0.531$  nm, and  $\beta_m = 99.25$  deg,<sup>[36,37]</sup> then  $\varphi$  and  $\alpha$  are predicted to be 0 and 76.49 deg, respectively. Therefore, the predicted orientation relationship is in the form  $(200)_m // (400)_o$ ,  $[0\bar{1}0]_m // [010]_o$ , and  $[00\bar{1}]_m // [001]_o$ , and the predicted monoclinic/orthorhombic interface is  $\sim 13.51$  deg clockwise away from the  $(400)_o$  plane, as indicated by the angle  $\beta$  in Figure 5(b). The unit height of the Moiré ledges is predicted to be  $\sim 1.59$  nm.

It is important to emphasize that  $a_o = 1.0166$  nm, rather than  $a_o = 1.014$  nm, is used in the present calculation, in order to make  $\eta_y = 1$ . The use of  $a_o = 1.014$  nm<sup>[36,37]</sup> leads to a slight counterclockwise rotation ( $\varphi = -0.035$  deg) of the monoclinic lattice, with respect to the orthorhombic lattice and thus a slight deviation from the otherwise rational orientation relationship. While this lattice rotation is quite small, it destroys the existence of a set of Moiré planes, such as that illustrated in Figure 5(b), in which the matching of  $(002)_m // (002)_o$  planes and of  $(200)_m // (400)_o$  planes can both occur in every plane of this set of Moiré planes. Figure 5(c) shows two identical variants of the monoclinic lattice generated from a single crystal of the orthorhombic lattice.<sup>[36]</sup> These two variants are separated by a single orthorhombic crystal, resulting in the formation of two orthorhombic/monoclinic interfaces that are parallel to each other. If the separation distance between these two orthorhombic/monoclinic

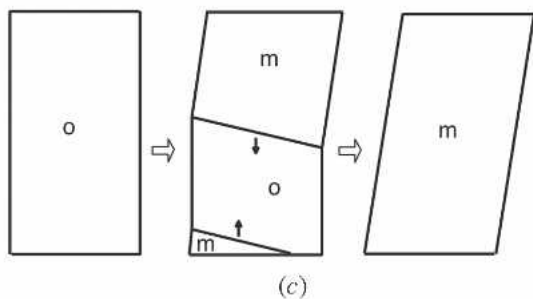
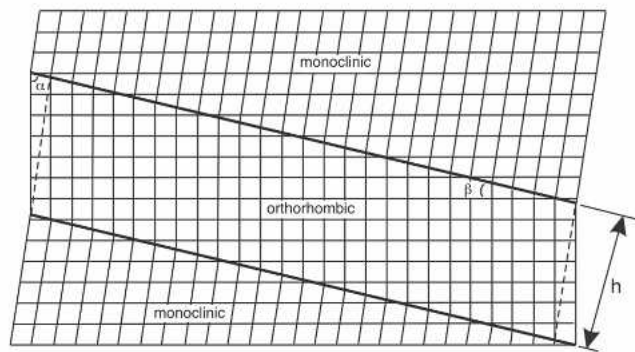
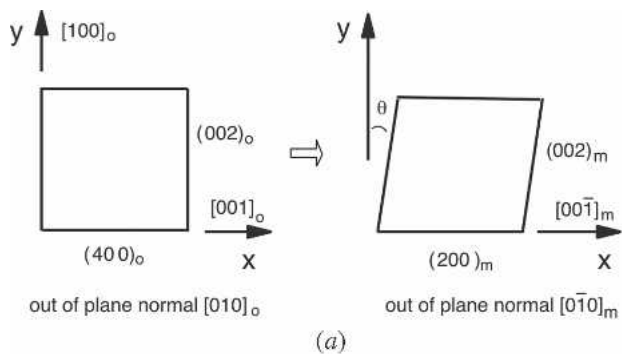


Fig. 5—Schematic diagrams showing (a) structural transformation from orthorhombic to monoclinic in zirconia, (b) matching of lattice planes in two parallel orthorhombic/monoclinic interfaces (Moiré planes) defined by the intersection of the  $(002)_m$  and  $(002)_o$  planes, and (c) shape change from a single crystal of orthorhombic to a single crystal of monoclinic.<sup>[36]</sup> Note that the separating distance between the two interfaces in (c) has to be a multiple of the interplanar spacing of the Moiré planes ( $h$ ) in order to generate a perfect single crystal of monoclinic.

interfaces is  $nh$ , where  $n$  is an integer number and  $h$  is the interplanar spacing of the Moiré planes defined by the intersection of the  $(002)_m$  and  $(002)_o$  planes, then the impingement of these two interfaces, due to their migration towards each other, will generate a perfect single crystal of the monoclinic lattice, as observed experimentally.<sup>[36]</sup>

The macroscopically planar interface depicted in Figure 5 was reported to adopt a form of structural disconnections (or structural ledges) and terraces, as shown in Figure 5 in Reference 36, with the terrace plane parallel to  $(200)_m$  or  $(400)_o$  planes. It was also suggested<sup>[36,41,42]</sup> that the macroscopic interface migrates in its normal direction *via* the cooperative gliding of the structural disconnections (termed “transformation dislocations” in Reference 36 and “coherency dislocations” in Reference 42) within the terrace plane. An alternative, and energetically favorable, mechanism for the migration of this planar interface is *via* the nucleation and lateral gliding

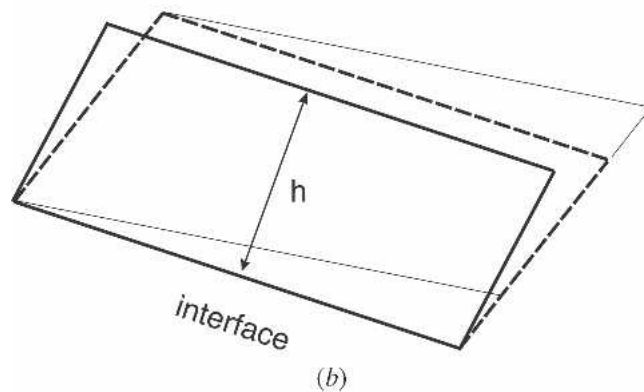
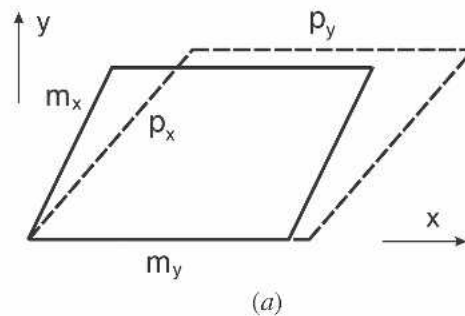


Fig. 6—(a) Schematic diagram showing the structural change defined by  $\eta_y \neq 1$ ,  $\eta_x \neq 1$ , and  $s \neq 0$ . (b) The (high-index) planar interface, the total lattice transformation (dashed line), and the shape change (hair line). The total lattice transformation can be described by a simple shear parallel to the interface and a uniaxial dilatation normal to the interface. The magnitude of dilatation strain normal to the interface is given by  $(\eta_x \eta_y - 1)$ .

of Moiré ledges,<sup>[1]</sup> the unit height of which is defined by the interplanar spacing of the Moiré planes resulting from the intersection of the  $(002)_m$  and  $(002)_o$  planes. These two distinctly different mechanisms can be distinguished either by direct *in-situ* transmission electron microscopy observations in the  $[0\bar{1}0]_m // [010]_o$  direction or by careful examination of the thickness variation of the transformation product, as the former mechanism leads to a continuous variation in thickness while the latter mechanism leads to a discrete variation in thickness. While there is a lack of sufficient and compelling experimental evidence to establish the operating mechanism of the interface migration, careful inspection of the transmission electron microscopy image in Figure 9(b) in Reference 36 reveals unambiguously the presence of an isolated ledge, on the macroscopically planar interface, that resembles the features of Moiré ledges.

### B. Interfaces Associated with Near-Rational Orientation Relationships

For structural transformations in which  $\eta_y \neq 1$  (and  $\eta_x \neq 1$ ) (Figure 6(a)), a single planar interface (fully coherent) can still exist, provided the product lattice is rotated through a proper angle  $\varphi$ , with respect to the matrix lattice (Eq. [1]). Since the rotation angle rarely has a value that leads to another rational orientation relationship, the orientation relationship between the two lattices is thus regarded as near rational, with the  $p_y$  plane deviated from the  $m_y$  plane by an angle of  $\varphi$ . The planar interface associated with this near-rational orientation relationship is often rotated away from the low-index plane

$m_y$  (Eq. [2]), and thus has a high index (Figure 6(b)). Note that commensurate edge-to-edge matching of the  $p_x$  and  $m_x$  planes and of the  $p_y$  and  $m_y$  planes cannot both be achieved in each individual plane in the set of Moiré planes defined by the intersection of the  $p_x$  and  $m_x$  planes. In this case, the total transformation strain (structural change plus lattice rotation) can be regarded as having a combination of a simple shear and a simple dilatation (Figure 6(b)), and is thus equivalent to that depicted in Figure 2(a). But the shape change is now different from that associated with a general shear (Figure 3(b)), due to the rotation of the product lattice.

While the high-index planar interface depicted in Figure 6(b) may again adopt a form of structural disconnections (or structural ledges) and terraces such as that depicted in Figure 4(c), its motion in the normal direction is expected to involve the nucleation and lateral gliding of growth ledges that are in the form of Moiré ledges. The formation of any ledges on this planar interface leads to an elastic distortion in the vicinity of the newly formed interface. While it is still possible to establish a coherent matching of lattice planes in the newly formed interface, when the value of  $\eta_y$  is close to unity, it is geometrically difficult for the transformation product to develop two broad surfaces that have an identical interface structure.

The only way to generate a transformation product that has two broad surfaces with identical interface structures is to invoke a lattice-invariant shear (LIS) on the  $p_x$  planes (Figure 7). The spacing of the planar defects of LIS is determined by the dilatation strain ( $\eta_y - 1$ ) of the structural transformation and the shear strain of the LIS. In segments between each two adjacent planar faults in the transformation product, the commensurate edge-to-edge matching of the  $p_x$  and  $m_x$  planes and of the  $p_y$  and  $m_y$  planes can be maintained, even though some elastic distortion of either or both lattices is involved.<sup>[43]</sup> Note that a shape change is also associated with the LIS, and that this LIS shape change makes the net macroscopic shape change of the transformation equivalent to that associated with a simple shear and a uniaxial dilatation. The resultant transformation product is expected to have two parallel-sided planar surfaces that are partially coherent. The migration of this partially coherent interface can again involve the nucleation and lateral sliding of the Moiré ledges within the Moiré plane interface, with the unit height of the Moiré ledges being defined by the intersection of the  $m_x$  and  $p_x$  planes.

Examples of planar interfaces in this group of structural transformations include broad surfaces of Cr laths/plates in

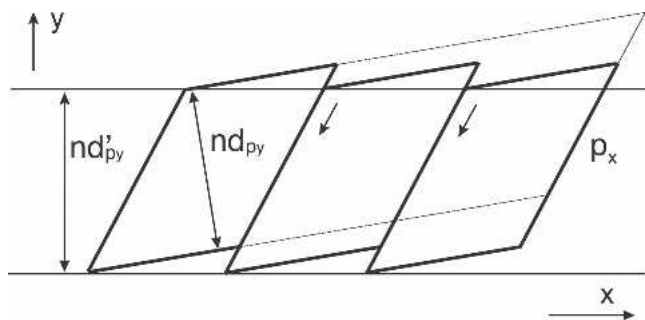


Fig. 7—Schematic diagram showing a change in interplanar spacing  $d_{p_y}$  due to the regular occurrence of LIS on plane  $p_x$ ;  $n$  is an integer. Note that a shape change is associated with the LIS.

the matrix of Cu, Ni, or Ti;<sup>[44–52]</sup> broad surfaces of  $\text{Mo}_5\text{Si}_3$  laths in  $\text{MoSi}_2$ ;<sup>[53]</sup> the habit plane of  $\text{Fe}_4\text{N}$  plates in Fe;<sup>[54,55]</sup> the side surface of  $\text{Mg}_{17}\text{Al}_{12}$  laths (with a near-Burgers orientation relationship) in Mg;<sup>[56,57]</sup> and the habit plane of the  $\alpha_1$  plates of a metastable 9R phase in a B2 matrix in Ag-Cd, Cu-Zn, and Cu-Zn-Al alloys.<sup>[14,58–61]</sup> Three high-resolution transmission electron microscopy images, showing commensurate edge-to-edge matching of closest- or near-closest-packed planes, are provided in Figure 8.

Studies using transmission electron microscopy<sup>[14,58]</sup> of the B2  $\Rightarrow$  9R transformation in Ag-Cd alloys reveal that the orientation relationship between 9R and B2 lattices is very close to rational, with  $(\bar{1}14)_{9R} \sim // (011)_{B2}$  and  $[110]_{9R} \sim // [1\bar{1}1]_{B2}$ .

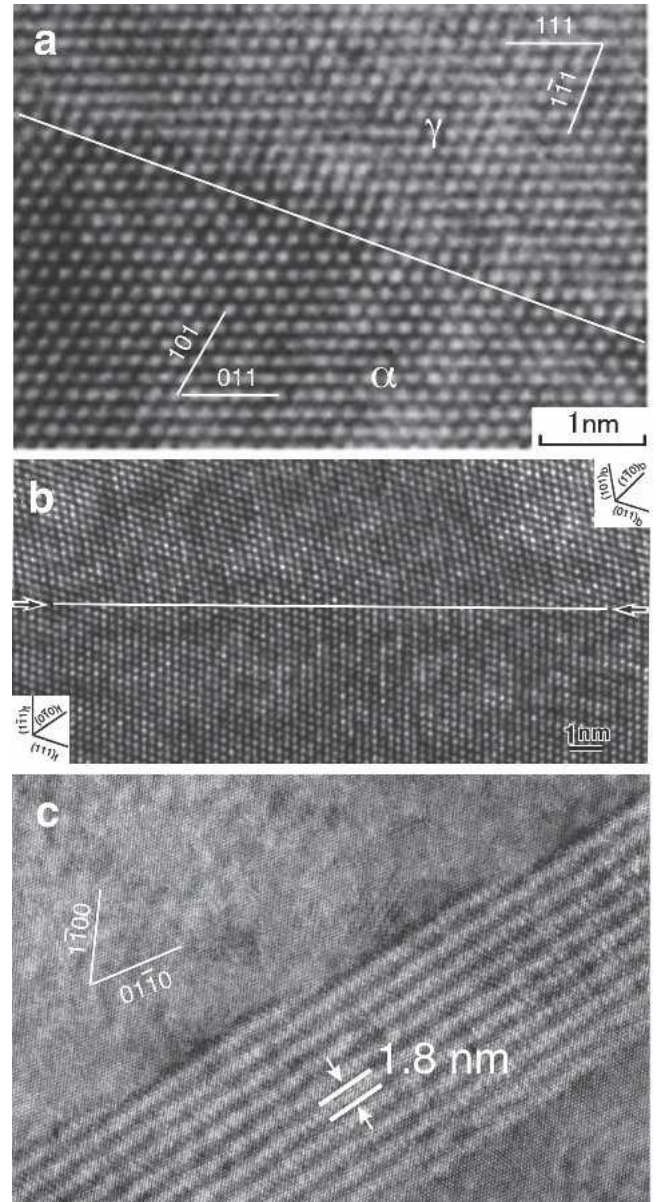


Fig. 8—High-resolution transmission electron microscopy images showing edge-to-edge matching of lattice planes in the planar interface of (a) a martensite lath in a Fe-Ni-Mn alloy in Reference 62 (courtesy of T. Furuhashi), (b) a martensite lath in a Fe-Ni-Co-Ti alloy in Reference 43 (courtesy of S. Kajiwara), and (c) a  $\text{Mg}_{17}\text{Al}_{12}$  lath in a Mg-9 wt pct Al alloy.<sup>[3]</sup> The planar interface is indicated by the white line in (a) and (b) and Moiré planes in (c).

The 9R product ( $\alpha_1$  plates) often has a parallel-sided plate morphology and a substructure of stacking faults that form on  $(009)_{9R}$  and are distributed regularly within the  $\alpha_1$  plate. The two broad surfaces (habit planes) of the  $\alpha_1$  plates are strikingly parallel to each other, and they are rotated  $\sim 6.5$  deg away from  $(011)_{B2}$ , toward  $(\bar{1}10)_{B2}$ .<sup>[14,58]</sup> An inspection of the 9R and B2 lattices in the  $[110]_{9R} // [11\bar{1}]_{B2}$  direction reveals that the 9R lattice can be generated from the B2 lattice by shearing and expanding the B2 lattice in the  $[\bar{2}1\bar{1}]_{B2}$  direction on  $(011)_{B2}$ , and by expanding it in the  $[011]_{B2}$  direction (Figure 9(a)). If we assume that  $a_{B2} = 0.293$  nm,  $a_{9R} = 0.444$  nm,  $b_{9R} = 0.264$  nm,  $c_{9R} = 1.921$  nm, and  $\beta_m = 89$  deg,<sup>[14]</sup> then the angle between planes  $(\bar{1}14)_{9R}$  and  $(009)_{9R}$  is 64.3 deg,

$$s = \tan(90 \text{ deg} - 64.3 \text{ deg}) - \tan(90 \text{ deg} - 60 \text{ deg}) = -0.096,$$

$$\eta_x = (d_{(009)_{9R}} \sin 60 \text{ deg}) / (d_{(011)_{B2}} \sin 64.3 \text{ deg}) = 0.990,$$

and

$$\eta_y = d_{(\bar{1}14)_{9R}} / d_{(\bar{1}10)_{B2}} = 0.986.$$

The values of  $\varphi$  and  $\beta$  are predicted to be 0.082 and 5.99 deg, respectively, where  $\beta$  is the angle between the AB interface and  $(011)_{B2}$ . The orientation relationship predicted by the theory is thus close to rational, and the predicted habit plane of the  $\alpha_1$  plates is  $\sim 6$  deg clockwise away from  $(011)_{B2}$ , when viewed along the  $[110]_{9R} // [11\bar{1}]_{B2}$  direction (Figure 9(b)). The predicted unit height of the Moiré ledges is  $\sim 2.65$  nm. It should be emphasized that the value of  $\varphi$  can reach

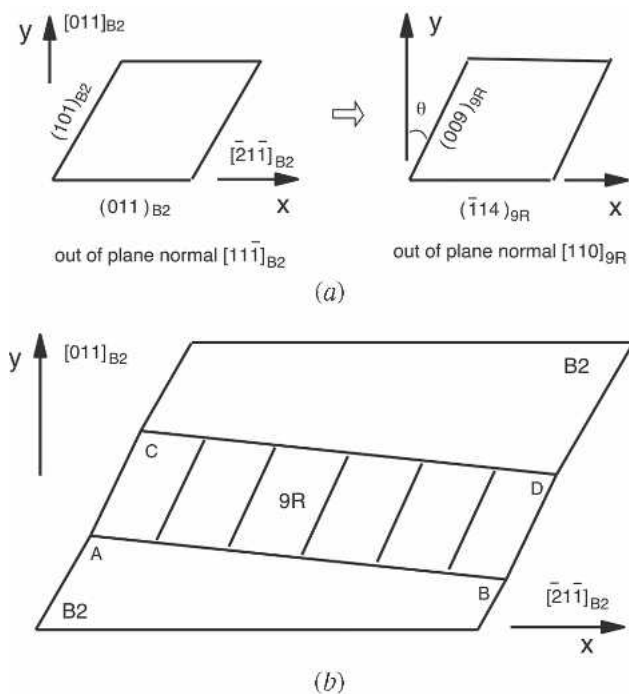


Fig. 9—Schematic diagrams showing (a) structural transformation from B2 (bcc) to 9R (monoclinic) in a Ag-45 at. pct Cd alloy, and (b) a parallel-sided plate of 9R in the B2 matrix. The thickness of this plate needs to be a multiple of the interplanar spacing of Moiré planes in order to have identical structure in the AB and CD interfaces.

zero if a small change is made on the lattice parameters of either the B2 or the 9R lattices. If the slight rotation of the 9R lattice, with respect to the B2 lattice, is accepted as representative, then LIS is required to generate a single plate that has identical structures on its two broad surfaces (Figure 9(b)). Similar to the planar interfaces discussed in Section IV, there is currently a lack of experimental evidence that would allow the operating mechanism of the interface migration to be established unambiguously. While some transmission electron microscopy evidence has been obtained for the existence of growth ledges on the habit plane of  $\alpha_1$  plates, and while it has been reported that the  $\alpha_1$  plates thicken *via* the nucleation and lateral sliding of growth ledges,<sup>[63]</sup> the crystallography and compatibility of such growth ledges with Moiré ledges, defined by the intersection of the  $(009)_{9R}$  and  $(101)_{B2}$  planes, are yet to be established.

## V. HIGH-INDEX PLANAR INTERFACES ASSOCIATED WITH IRRATIONAL ORIENTATION RELATIONSHIPS

Since the orientation relationship in this group of structural transformations is irrational (or random), the direction of the product lattice that is defined by the intersection of the  $p_x$  and  $p_y$  planes is thus irrationally oriented, with respect to the intersection line of the matrix lattice planes  $m_x$  and  $m_y$ . Under such circumstances, it is impossible to find even a single planar interface within which there exists an edge-to-edge matching of the  $m_x$  and  $p_x$  planes and of the  $m_y$  and  $p_y$  planes. However, the Moiré planes resulting from the intersection of the  $m_x$  and  $p_x$  planes and those defined by the intersection of the  $m_y$  and  $p_y$  planes still exist, and each of these two sets of Moiré planes may potentially become a planar interface; this is the case even though such a planar interface may be irrationally oriented with respect to either or both lattices, and thus has a high index. Any planar interfaces that adopt this configuration may represent a lower limit to the matching that is possible between the two lattices. It is conceivable that the motion of even such planar interfaces in their normal directions may still involve the nucleation and lateral gliding of Moiré ledges defined by the intersection of the  $m_x$  and  $p_x$  planes or of the  $m_y$  and  $p_y$  planes. One example is the planar facets of the massive  $\gamma_m$  phase in the  $\alpha_2$  matrix in a Ti-46.5 at. pct Al alloy. Existing experimental evidence suggests that the  $\gamma_m$  and  $\alpha_2$  lattices do not share a rational or close to rational orientation relationship, and that the planar  $\gamma_m/\alpha_2$  interfaces are irrationally oriented with respect to  $\alpha_2$  and  $\gamma_m$  lattices.<sup>[64-70]</sup> While such planar interfaces do not contain any linear defects,<sup>[67,68]</sup> recent studies using transmission electron microscopy<sup>[69]</sup> reveal that they are invariably parallel to the Moiré planes, defined by the intersection of two sets of closest-packed or near-closest packed planes in the  $\gamma_m$  and  $\alpha_2$  phases, as illustrated schematically in Figure 10. In irrational orientation relationships, the angle between the two sets of lattice planes is rarely zero; therefore, a shear displacement of one lattice with respect to the other is almost always associated with the motion of a planar interface, such as that depicted in Figure 10, even though it is now difficult to define whether a uniaxial dilatation is also associated with the motion of the planar interface.

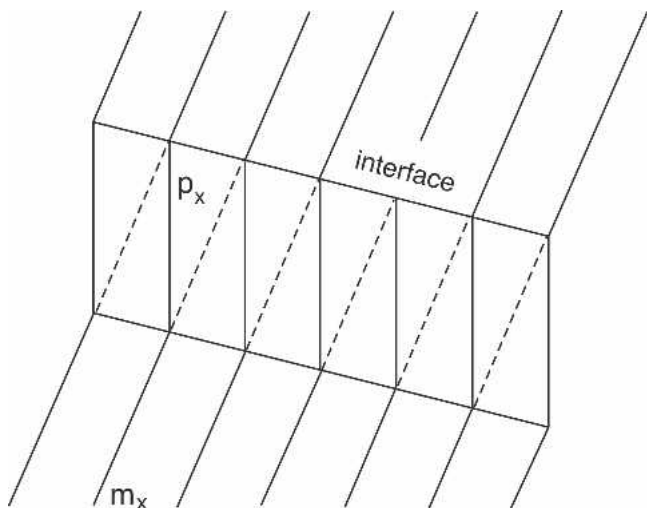


Fig. 10—Schematic diagram showing two sets of lattice planes that are related by a transformation of  $s \neq 0$ . The planar interface has a high index. Note that the uniaxial dilatation and the shape change cannot be defined, because only one set of planes from each lattice is involved in the lattice matching.

## VI. SUMMARY

For planar interfaces that are defined by the edge-to-edge matching of lattice planes, their crystallographic features and migration mechanisms can be coupled by the Moiré plane approach. On the basis of the features of the transformation strain, the planar interfaces are classified into three major groups, namely, (1) low-index interfaces associated with rational orientation relationships, (2) high-index interfaces associated with rational or near-rational orientation relationships, and (3) high-index interfaces associated with irrational orientation relationships.

- (1) For structural transformations without any expansions or contractions within the shear plane ( $\eta_x = 1$ ), the orientation relationship between the two lattices is invariably rational. A fully coherent planar interface always exists, and this interface is parallel to the (low-index) shear plane of the structural transformation. The migration of this low-index planar interface, in its normal direction, involves successive nucleation and lateral gliding of growth ledges, within the planar interface, that are often in the form of transformation disconnections. Such transformation disconnections are compatible with Moiré ledges, in terms of shape strain. A shape change is associated with the motion of the planar interface; this shape change can be either a simple shear ( $\eta_y = 1$ ) or a combination of a simple shear and a uniaxial dilatation ( $\eta_y \neq 1$ ).
- (2) For structural transformations with deformations within the shear plane ( $\eta_x \neq 1$ ), the orientation relationship between the two lattices is rational, if  $\eta_y = 1$ , or near-rational, if  $\eta_y \neq 1$ . In both cases, a fully coherent planar interface can exist, and this interface has a high index. Similar to the low-index interfaces, the high-index interface migrates in its normal direction again *via* successive nucleation and lateral gliding of growth ledges, now in the form of Moiré ledges, within the planar interface. The motion of the high-index interface also produces a shape change that can be described by a simple shear and a uni-

axial dilatation or a simple shear, a uniaxial dilatation, and a lattice rotation.

- (3) For a structural transformation that cannot be defined by a rational or near-rational orientation relationship (*i.e.*, irrational or random orientation relationship), it is always possible to identify a planar interface that is defined by the commensurate edge-to-edge matching of two sets of lattice planes. Similar to those planar interfaces that are associated with rational or near-rational orientation relationships, motion of a unidimensionally coherent interface in its normal direction may occur again *via* successive nucleation and lateral gliding of the Moiré ledges, and this interface motion produces a shape change that resembles the features of a shear.

## REFERENCES

1. J.F. Nie: *Acta Mater.*, 2004, vol. 52, pp. 795-807.
2. J.F. Nie: *Scripta Mater.*, 2005, vol. 52, pp. 687-91.
3. J.F. Nie: Monash University, Victoria, Australia, unpublished research.
4. J.M. Howe, H.I. Aaronson, and J.P. Hirth: *Acta Mater.*, 2000, vol. 48, pp. 3977-84.
5. J.W. Cahn and J.E. Taylor: *Acta Mater.*, 2004, vol. 52, pp. 4887-98.
6. H. Hashimoto, Y. Yokota, Y. Takai, H. Endoh, and A. Kumao: *Chemica Scripta*, 1978-79, vol. 14, pp. 125-28.
7. J.W. Christian: *Metall. Trans. A*, 1982, vol. 13A, pp. 509-38.
8. J.M. Penisson, M. Bacia, and T. Vystavel: *Interface Sci.*, 2004, vol. 12, pp. 175-86.
9. K.L. Merkle, L.J. Thompson, and F. Philipp: *Interface Sci.*, 2004, vol. 12, pp. 277-92.
10. K.L. Merkle, L.J. Thompson, and F. Philipp: *Phil. Mag. Lett.*, 2002, vol. 82, pp. 589-97.
11. J.W. Christian: *Metall. Mater. Trans. A*, 1994, vol. 25A, pp. 1821-39.
12. J.W. Christian: in *Martensite*, G.B. Olson and W.S. Owen, eds., ASM INTERNATIONAL, Materials Park, OH, 1992, pp. 103-23.
13. J.S. Bowles and C.M. Wayman: *Acta Metall.*, 1979, vol. 27, pp. 833-39.
14. B.C. Muddle, J.F. Nie, and G.R. Hugo: *Metall. Mater. Trans. A*, 1994, vol. 25A, pp. 1841-56.
15. H.I. Aaronson, T. Furuhashi, J.M. Rigsbee, W.T. Reynolds, and J.M. Howe: *Metall. Trans. A*, 1990, vol. 21A, pp. 2369-409.
16. H.I. Aaronson, B.C. Muddle, J.F. Nie, and J.P. Hirth: *Metall. Mater. Trans. A*, 2002, vol. 33A, pp. 2541-47.
17. J.P. Hirth: *Metall. Mater. Trans. A*, 1994, vol. 25A, pp. 1885-94.
18. J.P. Hirth and R.C. Pond: *Acta Mater.*, 1996, vol. 44, pp. 4749-63.
19. J.M. Howe, U. Dahmen, and R. Gronsky: *Phil. Mag. A*, 1987, vol. 56, pp. 31-61.
20. B.C. Muddle and I.J. Polmear: *Acta Metall.*, 1989, vol. 37, pp. 777-89.
21. R.W. Fonda, W.A. Cassada, and G.J. Shiflet: *Acta Metall. Mater.*, 1992, vol. 40, pp. 2539-46.
22. C.R. Hutchinson, X. Fan, S.J. Pennycook, and G.J. Shiflet: *Acta Mater.*, 2001, vol. 49, pp. 2827-41.
23. J.M. Howe, J. Lee, and A.K. Vasudevan: *Metall. Trans. A*, 1988, vol. 19A, pp. 2911-20.
24. U. Dahmen and K.H. Westmacott: *Phys. Status Solidi (a)*, 1983, vol. 80, pp. 249-62.
25. J.F. Nie and B.C. Muddle: *Acta Mater.*, 2000, vol. 48, pp. 1691-703.
26. J.L. Putaux and J.P. Chevalier: *Acta Mater.*, 1996, vol. 44, pp. 1701-16.
27. S. Kajiwaru: *Mater. Sci. Eng. A*, 1999, vol. A273-275, pp. 67-88.
28. S.R. Singh and J.M. Howe: *Phil. Mag. A*, 1992, vol. 66, pp. 739-71.
29. R. Bonnet, M. Loubradou, and U. Dahmen: *Phil. Mag. A*, 2000, vol. 80, pp. 2233-56.
30. J.M. Howe and D.A. Smith: *Acta Metall. Mater.*, 1992, vol. 40, pp. 2343-50.
31. J.F. Nye: *Physical Properties of Crystals*, Oxford University Press, London, 1957, p. 104.
32. J.B. Mitchell: *Acta Metall.*, 1971, vol. 19, pp. 1063-77.
33. K.H. Westmacott and U. Dahmen: in *Decomposition of Alloys: the Early Stages*, P. Haasen, V. Gerold, R. Wagner, and M.F. Ashby, eds., Pergamon Press, Oxford, United Kingdom, 1984, pp. 204-07.
34. P.M. Kelly and M.X. Zhang: *Mater. Forum*, 1999, vol. 23, pp. 41-62.



35. M. Sennour and C. Esnouf: *Acta Mater.*, 2003, vol. 51, pp. 943-57.
36. Y.H. Chiao and I.W. Chen: *Acta Metall. Mater.*, 1990, vol. 38, pp. 1163-74.
37. P.M. Kelly and L.R.F. Rose: *Progr. Mater. Sci.*, 2002, vol. 47, pp. 463-557.
38. R.H.J. Hannink, P.M. Kelly, and B.C. Muddle: *J. Am. Ceram. Soc.*, 2000, vol. 83, pp. 461-87.
39. G.R. Hugo, B.C. Muddle, and R.H.J. Hannink: *Mater. Sci. Forum*, 1988, vol. 34-36, pp. 165-69.
40. F.R. Chien, F.J. Uvic, V. Prakash, and A.H. Heuer: *Acta Mater.*, 1998, vol. 46, pp. 2151-71.
41. R.C. Pond and S. Celotto: *Int. Mater. Rev.*, 2003, vol. 48, pp. 225-45.
42. A.P. Sutton and R.W. Balluffi: *Interfaces in Crystalline Materials*, Oxford University Press, Oxford, United Kingdom, 1995, p. 539.
43. K. Ogawa and S. Kajiwara: *Phil. Mag.*, 2004, vol. 84, pp. 2919-47.
44. C.P. Luo and G.C. Weatherly: *Acta Metall.*, 1987, vol. 35, pp. 1963-72.
45. C.P. Luo, U. Dahmen, and K.H. Westmacott: *Acta Metall. Mater.*, 1994, vol. 42, pp. 1923-32.
46. C.P. Luo and U. Dahmen: *Acta Mater.*, 1998, vol. 46, pp. 2063-81.
47. J.K. Chen, G. Chen, and W.T. Reynolds: *Phil. Mag. A*, 1998, vol. 78, pp. 405-22.
48. G.J. Mahon, J.M. Howe, and S. Mahajan: *Phil. Mag. Lett.*, 1989, vol. 59, pp. 273-79.
49. G.C. Weatherly and W.Z. Zhang: *Metall. Mater. Trans. A*, 1994, vol. 25A, pp. 1865-74.
50. D. Qiu and W.Z. Zhang: *Phil. Mag.*, 2003, vol. 83, pp. 3093-116.
51. T. Furuhashi, J.M. Howe, and H.I. Aaronson: *Acta Metall. Mater.*, 1991, vol. 39, pp. 2873-86.
52. F. Ye, W.Z. Zhang, and D. Qiu: *Acta Mater.*, 2004, vol. 52, 2449-60.
53. S.Q. Xiao, S.A. Maloy, A.H. Heuer, and D. Dahmen: *Phil. Mag. A*, 1995, vol. 72, pp. 997-1013.
54. U. Dahmen, P. Ferguson, and K.H. Westmacott: *Acta Metall.*, 1987, vol. 35, pp. 1037-46.
55. U. Dahmen and K.H. Westmacott: *Acta Metall.*, 1986, vol. 34, pp. 475-82.
56. D. Duly, W.Z. Zhang, and M. Audier: *Phil. Mag. A*, 1995, vol. 71, pp. 187-204.
57. J.F. Nie, X.L. Xiao, C.P. Luo, and B.C. Muddle: *Micron*, 2001, vol. 32, pp. 857-63.
58. M.H. Wu, B.C. Muddle, and C.M. Wayman: *Acta Metall.*, 1988, vol. 36, pp. 2095-106.
59. Y. Nakata, T. Tadaki, and K. Shimizu: *Mater. Trans. JIM*, 1989, vol. 30, pp. 107-16.
60. K. Chattopadhyay and H.I. Aaronson: *Acta Metall.*, 1986, vol. 34, pp. 695-711.
61. M.H. Wu, J. Perkins, and C.M. Wayman: *Acta Metall.*, 1989, vol. 37, pp. 1821-37.
62. T. Moritani, N. Miyajima, T. Furuhashi, and T. Maki: *Scripta Mater.*, 2002, vol. 47, pp. 193-99.
63. N. Ravishankar, H.I. Aaronson, and K. Chattopadhyay: *Metall. Mater. Trans. A*, 1994, vol. 25A, pp. 2631-37.
64. H.I. Aaronson: *Metall. Mater. Trans. A*, 2002, vol. 33A, pp. 2285-97.
65. P. Wang, D. Veeraraghavan, M. Kumar, and V.K. Vasudevan: *Metall. Mater. Trans. A*, 2002, vol. 33A, pp. 2353-71.
66. J.M. Howe, W.T. Reynolds, and V.K. Vasudevan: *Metall. Mater. Trans. A*, 2002, vol. 33A, pp. 2391-411.
67. D. Veeraraghavan, P. Wang, and V.K. Vasudevan: *Acta Mater.*, 1999, vol. 47, pp. 3313-30.
68. J.F. Nie, B.C. Muddle, T. Furuhashi, and H.I. Aaronson: *Scripta Mater.*, 1998, vol. 39, pp. 637-45.
69. J.F. Nie and B.C. Muddle: *Metall. Mater. Trans. A*, 2002, vol. 33A, pp. 2381-89.
70. W.T. Reynolds, J.F. Nie, W.Z. Zhang, J.M. Howe, H.I. Aaronson, and G.R. Purdy: *Scripta Mater.*, 2003, vol. 49, pp. 405-09.